

CP in the Dark

Duarte Azevedo,^{1,2,*} Pedro M. Ferreira,^{3,1,†} M. Margarete Muhlleitner,^{4,‡}
Shruti Patel,^{4,5,§} Rui Santos,^{3,1,2,¶} and Jonas Wittbrodt^{6,**}

¹*Centro de Física Teórica e Computacional, Universidade de Lisboa, 1649-003 Lisboa, Portugal*

²*LIP, Departamento de Física, Universidade do Minho, 4710-057 Braga, Portugal*

³*Instituto Superior de Engenharia de Lisboa - ISEL, 1959-007 Lisboa, Portugal*

⁴*Institute for Theoretical Physics, Karlsruhe Institute of Technology, 76131 Karlsruhe, Germany*

⁵*Institute for Nuclear Physics, Karlsruhe Institute of Technology, 76344 Karlsruhe, Germany*

⁶*DESY, Notkestraße 85, 22607 Hamburg, Germany*

(Dated: October 8, 2018)

We build a model containing two scalar doublets and a scalar singlet with a specific discrete symmetry. After spontaneous symmetry breaking, the model has Standard Model-like phenomenology, as well as a hidden scalar sector which provides a viable dark matter candidate. We show that CP violation in the scalar sector occurs exclusively in the hidden sector, and consider possible experimental signatures of this CP violation. In particular, we study contribution to anomalous gauge couplings from the hidden scalars.

PACS numbers:

I. INTRODUCTION

The LHC discovery of a scalar with mass of 125 GeV [1, 2] completed the Standard Model particle content. The fact that precision measurements of the properties of this particle [3, 4] indicate that it behaves very much in a Standard Model (SM)-like manner is a further confirmation of the validity and effectiveness of that model. Nonetheless, the SM leaves a lot to be explained, and many extensions of the theory have been proposed to attempt to explain such diverse phenomena as the existence of dark matter, the observed universal matter-antimatter asymmetry and others. In particular, numerous SM extensions consist of enlarged scalar sectors, with singlets, both real and complex, being added to the SM Higgs doublet [5–13]; or doublets, the simplest example of which is the two-Higgs doublet model (2HDM) [14, 15]. Certain versions of singlet-doublet models provide dark matter candidates, as does the Inert version of the 2HDM (IDM) [16–30]. Famously, the 2HDM was introduced in 1973 by Lee to allow for the possibility of spontaneous CP violation. But models with dark matter candidates *and* extra sources of CP violation (other than the SM mechanism of CKM-matrix generated CP violation) are rare. Even rarer are models for which a “dark” sector exists, providing viable dark matter candidates, and where the extra CP violation originates exclusively in the “dark” sector. To the best of our knowledge, the only model with scalar CP violation in the dark sector is the recent work of Refs. [31, 32], for which a three-doublet model was considered. The main purpose of Refs. [31, 32] was to describe the dark matter properties of the model. In Ref. [33] an argument was presented to prove that the model is actually CP violating, adapting the methods of Refs. [34, 35] for the complex 2HDM (C2HDM).

In the current paper we will propose a model, simpler than the one in [31], but which boasts the same interesting properties, to wit: (a) a SM-like Higgs boson, h , “naturally” aligned due to the vacuum of the model preserving a discrete symmetry; (b) a viable dark matter candidate, the stability of which is guaranteed by the aforementioned vacuum and whose mass and couplings satisfy all existing dark matter search constraints; and (c) extra sources of CP

*E-mail: dazevedo@alunos.fc.ul.pt

†E-mail: pmmferreira@fc.ul.pt

‡E-mail: margarete.muehleitner@kit.edu

§E-mail: shruti.patel@kit.edu

¶E-mail: rasantos@fc.ul.pt

**E-mail: jonas.wittbrodt@desy.de

violation exist in the scalar sector of the model, but *only* in the “dark” sector. This *hidden* CP violation will mean that the SM-like scalar, h , behaves almost exactly like the SM Higgs boson, and in particular (unless contributions from a high number of loops are considered) h has couplings to gauge bosons and fermions which are exactly those of a scalar. This is all the more remarkable since the CP violation of the proposed model is *explicit*. The extra particle content of the model, as advertised, is simpler than the model of [31], consisting of two Higgs doublets (both of hypercharge $Y = 1$) and a real singlet ($Y = 0$). This is sometimes known as the Next-to-2HDM (N2HDM), and was the subject of a thorough study in [36]. The N2HDM version considered in this paper uses a different discrete symmetry than the symmetries considered in [36], designed, as will be shown, to produce both dark matter and dark CP violation. The paper is organised as follows: in section II we will introduce the model, explaining in detail its construction and symmetries, as well as the details of spontaneous symmetry breaking that occurs when one of the fields acquires a vacuum expectation value (vev). In section III we will present the results of a parameter space scan of the model, where all existing constraints – both theoretical and experimental (from colliders and dark matter searches) – are taken into account; deviations from the SM behaviour of h in the diphoton channel, stemming from the existence of a charged scalar, will be discussed, as will the contributions of the model to dark matter observables; in section IV we will discuss how CP violation arises in the dark sector, and how it might have a measurable impact in future colliders. Finally, we conclude in section V.

II. THE SCALAR POTENTIAL AND POSSIBLE VACUA

For our purposes, the N2HDM considered is very similar to that discussed in Ref. [36], in that the fermionic and gauge sectors are identical to the SM and the scalar sector is extended to include an extra doublet and also a singlet scalar field – thus the model boasts two scalar doublets, Φ_1 and Φ_2 , and a real singlet Φ_S . As in the 2HDM, we will require that the Lagrangian be invariant under a sign flip of some scalar fields, so that the number of free parameters of the model is reduced and no tree-level flavour-changing neutral currents (FCNC) occur [37, 38]. The difference between the current work and that of [36] consists in the discrete symmetry applied to the Lagrangian – here, we will consider a single Z_2 symmetry of the form

$$\Phi_1 \rightarrow \Phi_1 \quad , \quad \Phi_2 \rightarrow -\Phi_2 \quad , \quad \Phi_S \rightarrow -\Phi_S \quad . \quad (1)$$

With these requirements, the most general scalar potential invariant under $SU(2) \times U(1)$ is given by

$$\begin{aligned} V = & m_{11}^2 |\Phi_1|^2 + m_{22}^2 |\Phi_2|^2 + \frac{1}{2} m_S^2 \Phi_S^2 + \left(A \Phi_1^\dagger \Phi_2 \Phi_S + h.c. \right) \\ & + \frac{1}{2} \lambda_1 |\Phi_1|^4 + \frac{1}{2} \lambda_2 |\Phi_2|^4 + \lambda_3 |\Phi_1|^2 |\Phi_2|^2 + \lambda_4 |\Phi_1^\dagger \Phi_2|^2 + \frac{1}{2} \lambda_5 \left[\left(\Phi_1^\dagger \Phi_2 \right)^2 + h.c. \right] \\ & + \frac{1}{4} \lambda_6 \Phi_S^4 + \frac{1}{2} \lambda_7 |\Phi_1|^2 \Phi_S^2 + \frac{1}{2} \lambda_8 |\Phi_2|^2 \Phi_S^2 , \end{aligned} \quad (2)$$

where, with the exception of A , all parameters in the potential are real. As for the Yukawa sector, we consider all fermion fields *neutral* under this symmetry. As such, only the doublet Φ_1 couples to fermions, and the Yukawa Lagrangian is therefore

$$- \mathcal{L}_Y = \lambda_t \bar{Q}_L \tilde{\Phi}_1 t_R + \lambda_b \bar{Q}_L \Phi_1 b_R + \lambda_\tau \bar{L}_L \Phi_1 \tau_R + \dots \quad (3)$$

where we have only written the terms corresponding to the third generation of fermions, with the Yukawa terms for the remaining generations taking an analogous form. The left-handed doublets for quarks and leptons are denoted by Q_L and L_L , respectively; t_R , b_R and τ_R are the right-handed top, bottom and τ fields; and $\tilde{\Phi}_1$ is the charge conjugate of the doublet Φ_1 .

Notice that since the two doublets have the same quantum numbers and are not physical (only the mass eigenstates of the model will be physical particles), the potential must be invariant under basis changes on the doublets. This is a well-known property of 2HDMs, which the N2HDM inherits: any unitary transformation of these fields, $\Phi'_i = U_{ij} \Phi_j$ with a 2×2 unitary matrix U , is an equally valid description of the theory. Though the theory is invariant under such transformations, its parameters are not and undergo transformations dependent on U . A few observations are immediately in order:

- Since only Φ_1 has Yukawa interactions it must have a vev to give mass to all charged fermions¹. In fact the Yukawa sector of this model is identical to the one of the SM, and a CKM matrix arises there, as in the SM.

¹ And neutrinos as well, if one wishes to consider Dirac mass terms for them.

- The fact that all fermions couple to a single doublet, Φ_1 , automatically ensures that no scalar-mediated tree-level FCNC occur, as in the 2HDM with a Z_2 symmetry [37, 38].
- The Z_2 symmetry considered eliminates many possible terms in the potential, but does *not* force all of the remaining ones to be real – in particular, both the quartic coupling λ_5 and the cubic one, A , can be *a priori* complex. However, using the basis freedom to redefine doublets, we can absorb one of those complex phases into, for instance, Φ_2 . We choose, without loss of generality, to render λ_5 real.

A complex phase on A renders the model explicitly CP violating. Considering, for instance, the CP transformation of the scalar fields given by

$$\Phi_1^{CP}(t, \vec{r}) = \Phi_1^*(t, -\vec{r}) \quad , \quad \Phi_2^{CP}(t, \vec{r}) = \Phi_2^*(t, -\vec{r}) \quad , \quad \Phi_S^{CP}(t, \vec{r}) = \Phi_S(t, -\vec{r}) \quad , \quad (4)$$

we see that such a CP transformation, to be a symmetry of the potential, would require all of its parameters to be real. Notice that the CP transformation of the singlet trivially does not involve complex conjugation as Φ_S is real. In fact, this is a well-known CP property of singlet fields [39]. One point of caution is in order: the complex phase of A is not invariant under the specific CP transformation of Eq. (4), but by itself that does not prove that the model is explicitly CP violating. In fact, one could consider some form of generalized CP (GCP) transformation involving, other than complex conjugation of the fields, also doublet redefinitions: $\Phi_i^{GCP}(t, \vec{r}) = X_{ij} \Phi_j^*(t, -\vec{r})$. The model can only be said to be explicitly CP violating if there does not exist any CP transformation under which it is invariant. So, conceivably, though the model breaks the CP symmetry defined by the transformation of Eq. (4), it might be invariant under some other one. The point is moot, however: As we will see ahead, the vacuum of the model we will be considering is invariant under the CP transformation of Eq. (4) (and the Z_2 symmetry of Eq. (1)), but the theory has CP violation. Thus the CP symmetry was broken to begin with, and hence the model is explicitly CP violating.

Let us consider now the possibility of spontaneous symmetry breaking in which only the Φ_1 doublet acquires a neutral non-zero vev: $\langle \Phi_1 \rangle = (0, v/\sqrt{2})^T$. Given the structure of the potential in Eq. (2), the minimisation conditions imply that this is a possible solution, with all scalar components of the doublets (except the real, neutral one of Φ_1) and the singlet equal to zero, provided that the following condition is obeyed:

$$m_{11}^2 + \frac{1}{2} \lambda_1 v^2 = 0. \quad (5)$$

Since all fermion and gauge boson masses are therefore generated by Φ_1 , it is mandatory that $v = 246$ GeV as usual. At this vacuum, then, it is convenient to rewrite the doublets in terms of their component fields as

$$\Phi_1 = \begin{pmatrix} G^+ \\ \frac{1}{\sqrt{2}}(v + h + iG^0) \end{pmatrix} \quad , \quad \Phi_2 = \begin{pmatrix} H^+ \\ \frac{1}{\sqrt{2}}(\rho + i\eta) \end{pmatrix} \quad , \quad (6)$$

where h is the SM-like Higgs boson, with interaction vertices with fermions and gauge bosons identical to those expected in the SM (the diphoton decay of h , however, will differ from its SM counterpart). The mass of the h field is found to be given by

$$m_h^2 = \lambda_1 v^2 \quad , \quad (7)$$

and since $m_h = 125$ GeV, this fixes the value of one of the quartic couplings, $\lambda_1 \simeq 0.258$. The neutral and charged Goldstone bosons G^0 and G^+ , respectively, are found to be massless as expected, and the squared mass of the charged scalar H^+ is given by

$$m_{H^+}^2 = m_{22}^2 + \frac{\lambda_3}{2} v^2. \quad (8)$$

Finally, the two neutral components of the doublet Φ_2 , ρ and η , mix with the singlet component $\Phi_s \equiv s$ yielding a 3×3 mass matrix,

$$[M_N^2] = \begin{pmatrix} m_{22}^2 + \frac{1}{2} \bar{\lambda}_{345} v^2 & 0 & -\text{Im}(A) v \\ 0 & m_{22}^2 + \frac{1}{2} \lambda_{345} v^2 & \text{Re}(A) v \\ -\text{Im}(A) v & \text{Re}(A) v & m_S^2 + \frac{1}{2} \lambda_7 v^2 \end{pmatrix} \quad , \quad (9)$$

with $\bar{\lambda}_{345} = \lambda_3 + \lambda_4 - \lambda_5$ and $\lambda_{345} = \lambda_3 + \lambda_4 + \lambda_5$. There are therefore three neutral scalars other than h , which we call h_1 , h_2 and h_3 , in growing order of their masses. This mass matrix can then be diagonalized by an orthogonal rotation matrix R , such that

$$R M_N^2 R^T = \text{diag}(m_{h_1}^2, m_{h_2}^2, m_{h_3}^2) \quad (10)$$

and the connection between the original fields and the mass eigenstates is given by

$$\begin{pmatrix} h_1 \\ h_2 \\ h_3 \end{pmatrix} = R \begin{pmatrix} \rho \\ \eta \\ s \end{pmatrix}. \quad (11)$$

The rotation matrix R can be parametrized in terms of three angles, α_1 , α_2 and α_3 , such that

$$R = \begin{pmatrix} c_{\alpha_1} c_{\alpha_2} & s_{\alpha_1} c_{\alpha_2} & s_{\alpha_2} \\ -(c_{\alpha_1} s_{\alpha_2} s_{\alpha_3} + s_{\alpha_1} c_{\alpha_3}) & c_{\alpha_1} c_{\alpha_3} - s_{\alpha_1} s_{\alpha_2} s_{\alpha_3} & c_{\alpha_2} s_{\alpha_3} \\ -c_{\alpha_1} s_{\alpha_2} c_{\alpha_3} + s_{\alpha_1} s_{\alpha_3} & -(c_{\alpha_1} s_{\alpha_3} + s_{\alpha_1} s_{\alpha_2} c_{\alpha_3}) & c_{\alpha_2} c_{\alpha_3} \end{pmatrix}, \quad (12)$$

where for convenience we use the notation $c_i = \cos \alpha_i$, $s_j = \sin \alpha_j$. Without loss of generality, we may take the angles α_i in the interval $[-\pi/2, \pi/2]$.

In the following we discuss several phenomenological properties of this model. The vacuum preserves the Z_2 symmetry. As a result, the physical eigenstates emerging from Φ_2 and Φ_S , *i.e.* the charged scalar H^\pm and the neutral ones h_1 , h_2 and h_3 , carry a quantum number – a “dark charge” equal to -1 – which is preserved in all interactions, to all orders of perturbation theory. In the following we refer to these four eigenstates as “dark particles”. On the other hand, the SM-like particles (h , the gauge bosons and all fermions) have “dark charge” equal to 1 . The preservation of this quantum number means that dark particles must always be produced in pairs while in their decays they must always produce at least one dark particle. Therefore, the lightest of these dark particles – which we will choose in our parameter scans to be the lightest neutral state, h_1 – is *stable*. Thus, the model provides one dark matter candidate.

The model indeed shares many features with the Inert version of the 2HDM, wherein all particles from the “dark doublet” are charged under a discrete symmetry, the lightest of which is stable. The main difference with the current model is the mixing that occurs between the two neutral components of the doublet and the singlet due to the cubic coupling A , which can be appreciated from the mass matrix of Eq. (9). In what concerns the charged scalar, though, most of the phenomenology of this model is equal to the Inert 2HDM.

III. PARAMETER SCAN, THE DIPHOTON SIGNAL AND DARK MATTER OBSERVABLES

With the model specified, we can set about exploring its available parameter space, taking into account all of the existing theoretical and experimental constraints. We performed a vast scan over the parameter space of the model (100.000 different combinations of the parameters of the potential of Eq. (2)), requiring that:

- The correct electroweak symmetry breaking occurs, and the correct value for the mass of the observed Higgs boson is obtained; as already explained, this is achieved by requiring that $v = 246$ GeV in Eq. (6) while at the same time the parameters of the model are such that Eqs. (5) and (7) are satisfied.
- By construction, all tree-level interactions and vertices of the Higgs particle h are identical to those of the SM Higgs boson. As a consequence, all LHC production cross sections for h are identical to the values expected in the SM. Additionally, all decay widths of h , apart from the diphoton case to be treated explicitly below, are identical to their SM values up to electroweak corrections. This statement holds as we require the h_1 mass to be larger than roughly 70 GeV, to eliminate the possibility of the decay $h \rightarrow h_1 h_1$ (when this decay channel is open it tends to affect the branching ratios of h , making it difficult to have h be SM-like).
- The quartic couplings of the potential cannot be arbitrary. In particular, they must be such that the theoretical requirements of boundedness from below (BFB) – that the potential always tends to $+\infty$ along any direction where the scalar fields are taking arbitrarily large values – and perturbative unitarity – that the model remains both perturbative and unitary, in all $2 \rightarrow 2$ scalar scattering processes – are satisfied. The model considered in the current paper differs from the N2HDM discussed in Ref. [36] only via the cubic coefficient A , so the tree-level BFB and perturbative unitarity constraints described there (in sections 3.1 and 3.2) are exactly the ones we should use here.
- The constraints on the scalar sector arising from the Peskin-Takeuchi electroweak precision parameters S , T and U [40–42] are required to be satisfied in the model. Not much of the parameter space is eliminated due to this constraint, but it is still considered in full.
- Since the charged scalar H^\pm does not couple to fermions, all B -physics bounds usually constraining its interactions are automatically satisfied. The direct LEP bound of $m_{H^\pm} > 90$ GeV assumed a 100 % branching ratio of H^\pm to fermions, so that this constraint also needs not be considered here.

- The dark matter observables were calculated using `MicrOMEGAs` [43, 44] and compared to the results from Planck [45] and XENON1T [46].
- Since all scalars apart from h do not couple to fermions, no electric dipole moment constraints need be considered, this despite the fact that CP violation occurs in the model.

With these restrictions, the scan over the parameters of the model was such that:

- The masses of the neutral dark scalars h_1 and h_2 and the charged one, H^\pm , were chosen to vary between 70 and 1000 GeV. The last neutral mass, that of h_3 , is obtained from the remaining parameters of the model as explained in [36].
- The mixing angles of the neutral mass matrix, Eq. (12), were chosen at random in the interval $-\pi/2$ and $\pi/2$.
- The quartic couplings λ_2 and λ_6 are constrained, from BFB constraints, to be positive, and were chosen at random in the intervals $[0, 9]$ and $[0, 17]$, respectively. λ_8 is chosen in the interval $[-26, 26]$.
- The quadratic parameters m_{22}^2 and m_5^2 were taken between 0 and 10^6 GeV².

All other parameters of the model can be obtained from these using the expressions for the masses of the scalars and the definition of the matrix R . The scan ranges for the quartic couplings are chosen larger than the maximally allowed ranges after imposing unitarity and BFB. Therefore, all of the possible values for these parameters are sampled. We have used the implementation of the model, and all of its theoretical constraints, in `ScannerS` [47]. `N2HDECAY` [48], a code based on `HDECAY` [49, 50], was used for the calculation of scalar branching ratios and total widths, as in [36].

As we already explained, the tree-level interactions of h are identical to the ones of a SM Higgs boson of identical mass. The presence of the charged scalar H^\pm , however, changes the diphoton decay width of h , since a new loop, along with those of the W gauge boson and charged fermions, contributes to that width. This is identical to what occurs in the Inert model, and we may use the formulae of, for instance, Ref. [22]. Thus we find that the diphoton decay amplitude in our model is given by

$$\Gamma(h \rightarrow \gamma\gamma) = \frac{G_F \alpha^2 m_h^3}{128 \sqrt{2} \pi^3} \left| \sum_f N_{c,f} Q_f^2 A_{1/2} \left(\frac{4m_f^2}{m_h^2} \right) + A_1 \left(\frac{4m_W^2}{m_h^2} \right) + \frac{\lambda_3 v^2}{2m_{H^\pm}^2} A_0 \left(\frac{4m_{H^\pm}^2}{m_h^2} \right) \right|^2, \quad (13)$$

where the sum runs over all fermions (of electric charge Q_f and number of colour degrees of freedom $N_{c,f}$) and A_0 , $A_{1/2}$ and A_1 are the well-known form factors for spin 0, 1/2 and 1 particles (see for instance Refs. [51, 52]). The charged Higgs contribution to the diphoton amplitude in Eq. (13) changes this decay width, and therefore the total decay width, hence all branching ratios, of h with respect to the SM expectation. However, the diphoton decay width being so small compared to the main decay channels for h ($b\bar{b}$, ZZ and WW), the overall changes of the total h width are minimal. In fact, numerical checks for our allowed parameter points have shown that the branching ratios of h to $b\bar{b}$, $\tau\bar{\tau}$, ZZ and WW change by less than 0.05% compared to the corresponding SM quantities – therefore, all current LHC constraints for the observed signal rates of h in those channels are satisfied at the 1σ level.

As for the branching ratio into two photons, it can and does change by larger amounts, as can be appreciated from Fig. 1. In that figure we plot the ratio of the branching ratio of h into two photons to its SM value as a function of the charged Higgs mass. Comparing these results to the recent measurements of the $h \rightarrow \gamma\gamma$ signal rates² $\mu_{\gamma\gamma}$ from Ref. [53], we see that our model can accommodate values well within the 2σ interval. The lower bound visible in Fig. 1 emerges from the present experimental lower limit from [53] at 2σ . The experimental upper limit, however, is larger than the maximum value of ~ 1.2 possible in our model. The latter results from the combination of BFB and unitarity bounds which constrain the allowed values of the coupling λ_3 . The lowest allowed value for λ_3 , which governs the coupling of hH^+H^- , is about -1.03 , and its maximum one roughly 8.89. Since the value of $\mu_{\gamma\gamma}$ grows for negative λ_3 , the lower bound on λ_3 induces an upper bound of $\mu_{\gamma\gamma} \lesssim 1.2$.

Thus we see that the model under study in this paper is perfectly capable of reproducing the current LHC data on the Higgs boson. Specific predictions for the diphoton signal rate are also possible in this model – values of $\mu_{\gamma\gamma}$ larger or smaller than unity are easily accommodated, though they are constrained to the interval $0.917 \lesssim \mu_{\gamma\gamma} \lesssim 1.206$. As

² Notice that since h in this model has exactly the same production cross sections as the SM Higgs boson, the ratio of branching ratios presented in Fig. 1 corresponds exactly to the measured signal rate, which involves the ratio of the product of production cross sections and decay branching ratios, between observed and SM theoretical values.

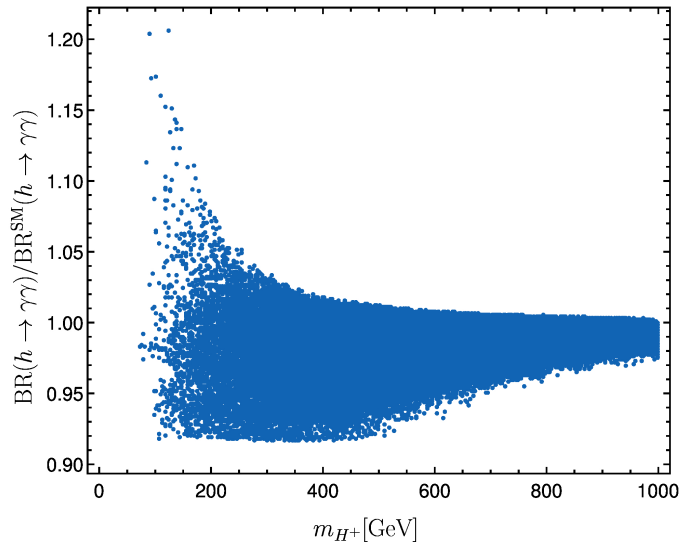


FIG. 1: Ratio of the branching ratio of h into two photons to the SM value *versus* the value of the charged scalar mass for all the allowed points in the model.

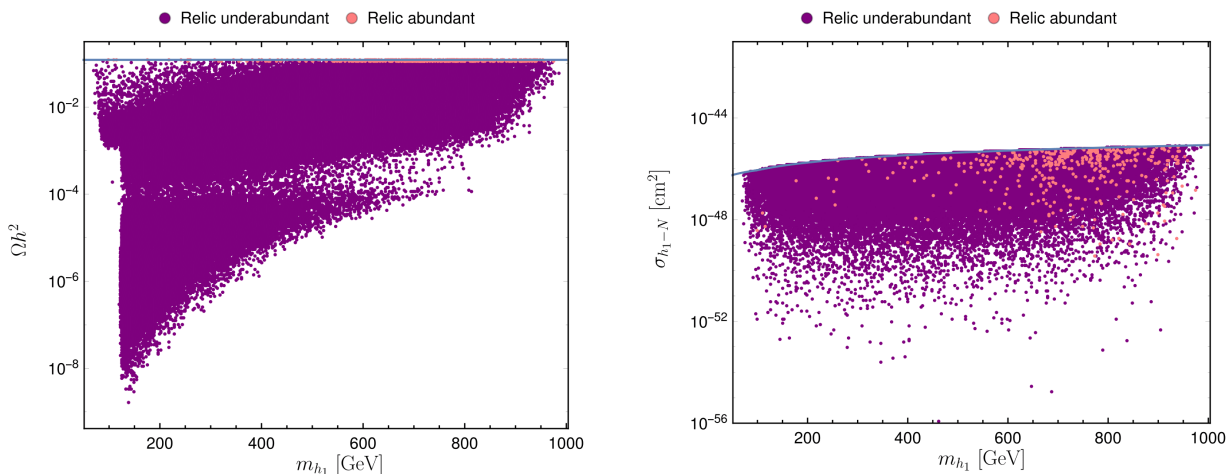


FIG. 2: Points that survive all experimental and theoretical constraints. Left: relic density abundance versus dark matter mass where the grey line represents the measured DM relic abundance; points either saturate the relic abundance constraints within $+1\sigma$ and -5σ around the central value (pink points) or are below the measured central value (violet points). Right: spin-independent nucleon dark matter scattering cross section as a function of the dark matter mass where the grey line represents the latest XENON1T [46, 54] results; colour code is the same and pink points are superimposed on violet points.

the parameter scan was made taking into account all data from dark matter searches, we are comfortable that all phenomenology in that sector is satisfied by the dark particles.

Let us now study how the model behaves in terms of dark matter variables. Several experimental results put constraints on the mass of the dark matter (DM) candidate, and on its couplings to SM particles. The most stringent bound comes from the measurement of the cosmological DM relic abundance from the latest results from the Planck Collaboration [45], $(\Omega h^2)_{\text{DM}}^{\text{obs}} = 0.120 \pm 0.001$. The DM relic abundance for our model was calculated with **MicrOMEGAs** [44]. In our scan we accepted all points that do not exceed the value measured by Planck by more than 1σ . This way, we consider not only the points that are in agreement with the DM relic abundance experimental values but also the points that are underabundant and would need further dark matter candidates to saturate the measured

experimental value.

Another important constraint comes from direct detection experiments, in which the elastic scattering of DM off nuclear targets induces nucleon recoils that are being measured by several experimental groups. Using the expression for the spin-independent DM-nucleon cross section given by MicrOMEGAS, we impose the most restrictive upper bound on this cross section, which is the one from XENON1T [46, 54].

In the left panel of Fig. 2 we use the parameter scan previously described to compute dark matter observables. We show the points that passed all experimental and theoretical constraints in the relic abundance versus dark matter mass plane. We present in pink the points that saturate the relic abundance, that is the points that are in the interval between $+1\sigma$ and -5σ around the central value, and in violet the points for which the relic abundance is below the measured value. It is clear that there are points in the chosen dark matter mass range that saturate the relic density. In the right panel we present the spin-independent nucleon dark matter scattering cross section as a function of the dark matter mass. The upper bound (the grey line) represents the latest XENON1T [46, 54] results. The pink points in the right plot show that even if the direct bound improves by a few orders of magnitude there will still be points for the entire mass range where the relic density is saturated.

Thus we see that the model under study in this paper can fit, without need for fine tuning, the existing dark matter constraints. Next we will study the rise of CP violation in the dark sector.

IV. CP VIOLATION IN THE DARK SECTOR

As we explained in section II, the model explicitly breaks the CP symmetry defined in Eq. (4). Notice that the vacuum of the model which we are studying – wherein only Φ_1 acquires a vev – preserves that symmetry. Therefore, if there is CP violation (CPV) in the interactions of the physical particles of the model, it did not arise from any spontaneous CPV, but rather the explicit CP breaking mentioned above³.

There are several eventual experimental observables where one could conceivably observe CPV. For instance, a trivial calculation shows that all vertices of the form Zh_ih_j , with $i \neq j$, are possible. These vertices arise from the kinetic terms for Φ_2 where from Eq. (6) we obtain, in terms of the neutral components of the second doublet,

$$|D_\mu \Phi_2|^2 = \dots + \frac{g}{\cos \theta_W} Z_\mu (\eta_2 \partial^\mu \rho_2 - \rho_2 \partial^\mu \eta_2), \quad (14)$$

where g is the $SU(2)_L$ coupling constant and θ_W is the Weinberg angle. With the rotation matrix between field components and neutral eigenstates defined in Eq. (12), we easily obtain ($i, j = 1, 2, 3$)

$$|D_\mu \Phi_2|^2 = \dots + \frac{g}{\cos \theta_W} (R_{ij} R_{ji} - R_{ii} R_{jj}) Z_\mu (h_i \partial^\mu h_j - h_j \partial^\mu h_i). \quad (15)$$

Thus decays or production mechanisms of the form $h_j \rightarrow Z h_i$, $Z \rightarrow h_j h_i$, for any $h_{i \neq j}$ dark neutral scalars, are *simultaneously* possible (with the Z boson possibly off-shell) which would clearly not be possible if the h_i had definite CP quantum numbers – in fact, due to CP violation, the three dark scalars are neither CP-even nor CP-odd, but rather states with mixed CP quantum numbers. The *simultaneous* existence of all $Zh_j h_i$ vertices, with $i \neq j$, is a clear signal of CPV in the model, in clear opposition to what occurs, for instance, in the CP-conserving 2HDM – in that model $Z \rightarrow A h$ or $Z \rightarrow A H$ are possible because A is CP-odd and h, H are CP-even, but $Z \rightarrow H h$ or $Z \rightarrow A A$ are forbidden. Since in our model all vertices $Zh_j h_i$ with $i \neq j$ occur, the neutral scalars h_i cannot have definite CP quantum numbers. Thereby CP violation is established in the model in the dark sector. Notice that no vertices of the form Zhh_i are possible. This is not due to any CP properties, however, but rather to the conservation of the Z_2 quantum number. Thus observation of such decays or production mechanisms (all three possibilities for $Z \rightarrow h_j h_i$, $i \neq j$, would have to be confirmed) could serve as confirmation of CPV in the model, though the non-observability of the dark scalars would mean they would only contribute to missing energy signatures. Both at the LHC and at future colliders, hints on the existence of dark matter can appear in mono- Z or mono-Higgs searches. The current model predicts cascade processes such as $q\bar{q}(e^+e^-) \rightarrow Z^* \rightarrow h_1 h_2 \rightarrow h_1 h_1 Z$ and $q\bar{q}(e^+e^-) \rightarrow Z^* \rightarrow h_1 h_2 \rightarrow h_1 h_1 h_{125}$, leading to mono- Z and mono-Higgs events, respectively. This type of final states occurs in many dark matter models,

³ Again, because this is a subtlety of CP symmetries, let us repeat the argument: The fact that the model explicitly violates one CP symmetry – that defined in Eq. (4) – does not necessarily mean there is CPV, since the Lagrangian could be invariant under a different CP symmetry. If, however, we prove that there is CPV after spontaneous symmetry breaking with a vacuum that preserves the CP symmetry of Eq. (4), then that CPV is explicit.

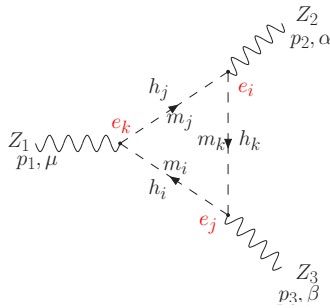


FIG. 3: Feynman diagram contributing to the CP violating form factor f_4^Z .

regardless of the CP-nature of the particles involved. Therefore, these are not good processes to probe CP-violation in the dark sector.

However, though CPV occurs in the dark sector of the theory, it can have an observable impact on the phenomenology of the SM particles. A sign of CPV in the model – possibly the only type of signs of CPV which might be observable – can be gleaned from the interesting work of Ref. [34] (see also Ref. [35]), wherein 2HDM contributions to the triple gauge boson vertices ZZZ and ZW^+W^- were considered. A Lorentz structure analysis of the ZZZ vertex, for instance [55–58], reveals that there are 14 distinct structures, which can be reduced to just two form factors on the assumption of two on-shell Z bosons and massless fermions, the off-shell Z being produced by e^+e^- collisions. Under these simplifying assumptions, the ZZZ vertex function becomes (e being the unit electric charge)

$$e\Gamma_{ZZZ}^{\alpha\beta\mu} = ie \frac{p_1^2 - m_Z^2}{m_Z^2} \left[f_4^Z \left(p_1^\alpha g^{\mu\beta} + p_1^\beta g^{\mu\alpha} \right) + f_5^Z \epsilon^{\mu\alpha\beta\rho} (p_2 - p_3)_\rho \right], \quad (16)$$

where p_1 is the 4-momentum of the off-shell Z boson, p_2 and p_3 those of the remaining (on-shell) Z bosons. The dimensionless f_4^Z form factor is CP violating, but the f_5^Z coefficient preserves CP. In our model there is only one-loop diagram contributing to this form factor, shown in Fig. 3. As can be inferred from the diagram there are three different neutral scalars circulating in the loop – in fact, the authors of Ref. [34] showed that in the 2HDM with explicit CPV (the C2HDM) the existence of at least three neutral scalars with different CP quantum numbers that mix among themselves is a necessary condition for non-zero values for f_4^Z . Notice that in the C2HDM there are *three* diagrams contributing to f_4^Z – other than the diagram shown in Fig. 3, the C2HDM calculation involves an additional diagram with an internal Z boson line in the loop, and another, with a neutral Goldstone boson G^0 line in the loop. In our model, however, the discrete Z_2 symmetry we imposed forbids the vertices ZZh_j and ZG^0h_i (these vertices do occur in the C2HDM, being allowed by that model’s symmetries), and therefore those two additional diagrams are identically zero. In [34] an expression for f_4^Z in the C2HDM was found, which can easily be adapted to our model, by only keeping the contributions corresponding to the diagram of Fig. 3. This results in

$$f_4^Z(p_1^2) = -\frac{2\alpha}{\pi s_{2\theta_w}^3} \frac{m_Z^2}{p_1^2 - m_Z^2} f_{123} \sum_{i,j,k} \epsilon_{ijk} C_{001}(p_1^2, m_Z^2, m_Z^2, m_i^2, m_j^2, m_k^2), \quad (17)$$

where α is the electromagnetic coupling constant and the `LoopTools` [59] function C_{001} is used. The f_{123} factor denotes the product of the couplings from three different vertices, given in Ref. [34] by

$$f_{123} = \frac{e_1 e_2 e_3}{v^3}, \quad (18)$$

where the $e_{i,j,k}$ ($i, j, k = 1, 2, 3$) factors, shown in Fig. 3, are related to the coupling coefficients that appear in the vertices $Zh_i h_j$ (in the C2HDM they also concern the $ZG^0 h_i$ and ZZh_i vertices, *cf.* [35]). With the conventions of the current paper, we can extract these couplings from Eq. (15) and it is easy to show that

$$\begin{aligned} f_{123} &= (R_{12}R_{21} - R_{11}R_{22}) (R_{13}R_{31} - R_{11}R_{33}) (R_{23}R_{32} - R_{22}R_{33}) \\ &= R_{13}R_{23}R_{33}, \end{aligned} \quad (19)$$

where the simplification that led to the last line originates from the orthogonality of the R matrix. We observe that the maximum value that f_{123} can assume is $(1/\sqrt{3})^3$, corresponding to the *maximum mixing* of the three neutral components, ρ , η and $\Phi_S \equiv s$. This is quite different from what one expects to happen in the C2HDM, for instance – there one of the mixed neutral states is the observed 125 GeV scalar, and its properties are necessarily very SM-like,

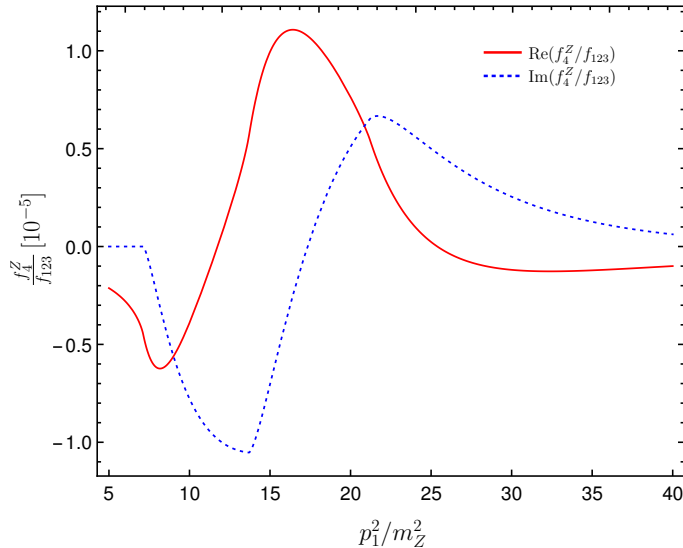


FIG. 4: The CP-violating $f_4^Z(p_1^2)$ form factor, normalized to f_{123} , for $m_{h_1} = 80.5$ GeV, $m_{h_2} = 162.9$ GeV and $m_{h_3} = 256.9$ GeV, as a function of the squared off-shell Z boson 4-momentum p_1^2 , normalized to m_Z^2 .

which implies that the 3×3 matrix R should approximately have the form of one diagonal element with value close to 1, the corresponding row and column with elements very small and a 2×2 matrix mixing the other eigenstates⁴. Within our model, however, the three neutral dark fields can mix as much or as little as possible.

In Fig. 4 we show, for a random combination of dark scalar masses ($m_{h_1} \simeq 80.5$ GeV, $m_{h_2} \simeq 162.9$ GeV and $m_{h_3} \simeq 256.9$ GeV) the evolution of f_4^Z normalized to f_{123} ⁵ with p_1^2 , the 4-momentum of the off-shell Z boson. This can be compared with Fig. 2 of Ref. [34], where we see similar (if a bit larger) magnitudes for the real and imaginary parts of f_4^Z , despite the differences in masses for the three neutral scalars in both situations (in that figure, the masses taken for h_1 and h_3 were, respectively, 125 and 400 GeV, and several values for the h_2 mass were considered). As can be inferred from Fig. 4, f_4^Z is at most of the order of $\sim 10^{-5}$. For the parameter scan described in the previous section, we obtain, for the imaginary part of f_4^Z , the values shown in Fig. 5. We considered two values of p_1^2 (corresponding to two possible collision energies for a future linear collider). The imaginary part of f_4^Z (which, as we will see, contributes directly to CP-violating observables such as asymmetries) is presented as a function of the overall coupling f_{123} defined in Eq. (19). We in fact present results as a function of $f_{123}/(1/\sqrt{3})^3$, to illustrate that indeed the model perfectly allows maximum mixing between the neutral, dark scalars. Fig. 5 shows that the maximum values for $|\text{Im}(f_4^Z)|$ are reached for the maximum mixing scenarios. We also highlight in red the points for which the dark neutral scalars h_i have masses smaller than 200 GeV. The loop functions in the definition of f_4^Z , Eq. (17), have a complicated dependence on masses (and external momentum p_1) so that an analytical demonstration is not possible, but the plots of Fig. 5 strongly imply that choosing all dark scalar masses small yields smaller values for $|\text{Im}(f_4^Z)|$. Larger masses, and larger mass splittings, seem to be required for larger $|\text{Im}(f_4^Z)|$. A reduction on the maximum values of $|\text{Im}(f_4^Z)|$ (and $|\text{Re}(f_4^Z)|$) with increasing external momentum is observed (though that variation is not linear, as can be appreciated from Fig. 4). A reduction of the maximum values of $|\text{Im}(f_4^Z)|$ (and $|\text{Re}(f_4^Z)|$) when the external momentum tends to infinity is also observed.

The smaller values for $|\text{Im}(f_4^Z)|$ for the red points can be understood in analogy with the 2HDM. The authors of Ref. [34] argue that the occurrence of CPV in the model implies a non-zero value for the basis-invariant quantities introduced in Refs. [60, 61], in particular for the imaginary part of the J_2 quantity introduced therein. Since $\text{Im}(J_2)$ is proportional to the product of the differences in mass squared of all neutral scalars, having all those scalars with lower masses and lower mass splittings reduces $\text{Im}(J_2)$ and therefore the amount of CPV in the model. Now, in our model the CPV basis invariants will certainly be different from those of the 2HDM, but we can adapt the argument to

⁴ Meaning, a neutral scalar mixing very similar to the CP-conserving 2HDM, where h and H mix via a 2×2 matrix but A does not mix with the CP-even states.

⁵ For this specific parameter space point, we have $f_{123} \simeq -0.1835$.

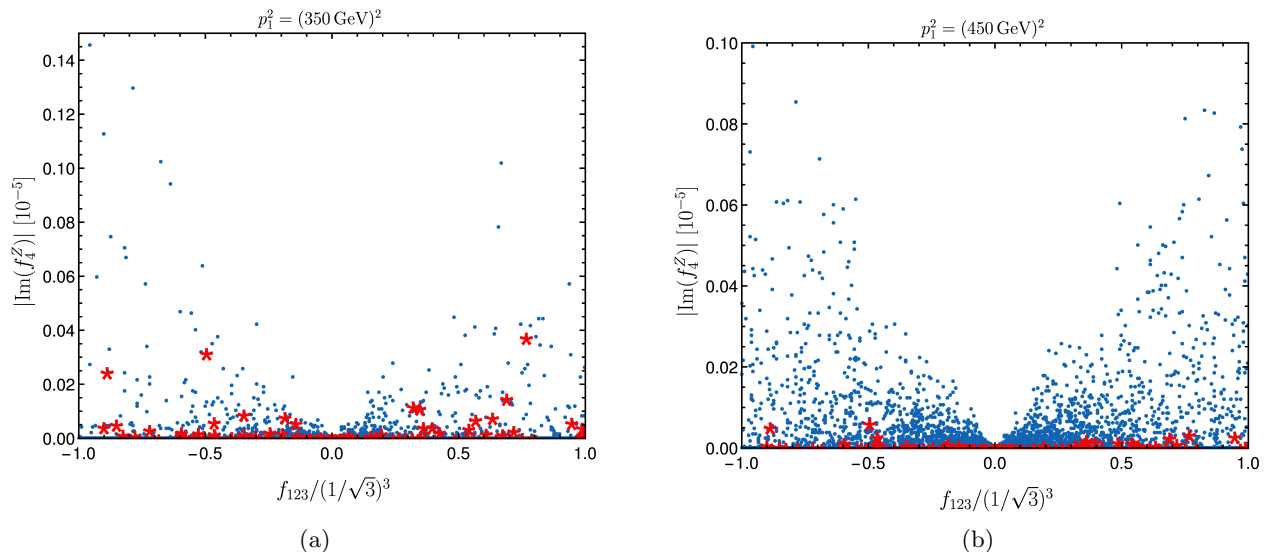


FIG. 5: Scatter plots for the imaginary part of f_4^Z as a function of the combined Z -scalars coupling f_{123} of Eq. (19), divided by its maximum possible value of $(1/\sqrt{3})^3$. In (a) results for $p_1^2 = (350 \text{ GeV})^2$; in (b), $p_1^2 = (450 \text{ GeV})^2$. In red, points for which the masses of all the dark scalars are smaller than 200 GeV, $m_{h_i} < 200 \text{ GeV}$ ($i = 1, 2, 3$).

understand the behaviour of the red points in Fig. 5: those red points correspond to three dark neutral scalars with masses lower than 200 GeV, and therefore their mass splittings will be small (compared to the remaining parameter space of the model). In the limiting case of three degenerate dark scalars, the mass matrix of Eq. (9) would be proportional to the identity matrix and therefore no mixing between different CP states would occur. With this analogy, we can understand how regions of parameter space with larger mass splittings between the dark neutral scalars tend to produce larger values of $|\text{Im}(f_4^Z)|$.

Experimental collaborations have been probing double- Z production to look for anomalous couplings such as those responsible for a ZZZ vertex [62–70]. The search for anomalous couplings in those works uses the effective Lagrangian for triple neutral vertices proposed in Ref. [55], parametrised as

$$\mathcal{L}_{VZZ} = -\frac{e}{m_Z^2} \left\{ [f_4^\gamma (\partial_\mu F^{\mu\alpha}) + f_4^Z (\partial_\mu Z^{\mu\alpha})] Z_\beta (\partial^\beta Z_\alpha) - [f_5^\gamma (\partial^\mu F_{\mu\alpha}) + f_5^Z (\partial^\mu Z_{\mu\alpha})] \tilde{Z}^{\alpha\beta} Z_\beta \right\}, \quad (20)$$

where γZZ vertices were also considered. In this equation, $F_{\mu\nu}$ is the electromagnetic tensor, $Z_{\mu\nu} = \partial_\mu Z_\nu - \partial_\nu Z_\mu$ and $\tilde{Z}_{\mu\nu} = \epsilon_{\mu\nu\rho\sigma} Z^{\rho\sigma}/2$. The f_4^Z coupling above is taken to be a constant, and as such it represents at most an approximation to the $f_4^Z(p_1^2)$ of Eq. (17). Further, the analyses of the experimental collaborations mentioned above take this coupling to be real, whereas the imaginary part of $f_4^Z(p_1^2)$ is the quantity of interest in many interesting observables. With all that under consideration, latest results from LHC [70] already probe the f_4^Z coupling of Eq. (20) to order $\sim 10^{-3}$, whereas the typical magnitude of $f_4^Z(p_1^2)$ (both real and imaginary parts) is $\sim 10^{-5}$. We stress, however, that the two quantities cannot be directly compared, as they represent very different approaches to the ZZZ vertex. A thorough study of the experimental results of [70] using the full expression for the ZZZ vertex of Eq. (16) and the full momentum (and scalar masses) dependence of the form factors is clearly necessary, but beyond the scope of the current work.

The crucial aspect to address here, and the point we wish to make with the present section, is that $f_4^Z(p_1^2)$ is non-zero in the model under study in this paper. Despite the fact that the neutral scalars contributing to the form factor are all dark particles, CP violation is therefore present in the model and it can indeed be “visible” to us, having consequences in the non-dark sector. We also analysed other vertices, such as ZW^+W^- – there CPV form factors also arise, also identified as “ f_4^Z ”, and for our parameter scan we computed it by once again adapting the results of Ref. [34] to our model. In the C2HDM three Feynman diagrams contribute to this CP-violating form factor (see Fig. 17 in [34]) but in our model the Z_2 symmetry eliminates the vertices $h_i W^+ W^-$ and $h_i G^+ W^-$, so only one diagram involving the charged scalar survives. From Eq. (4.4) of Ref. [34], we can read the expression of the CP-violating form factor f_4^Z from the ZW^+W^- vertex, obtaining

$$f_4^Z(p_1^2) = \frac{\alpha}{\pi s_{2\theta_W}^2} f_{123} \sum_{i,j,k} \epsilon_{ijk} C_{001}(p_1^2, m_W^2, m_W^2, m_i^2, m_j^2, m_{H^\pm}^2). \quad (21)$$

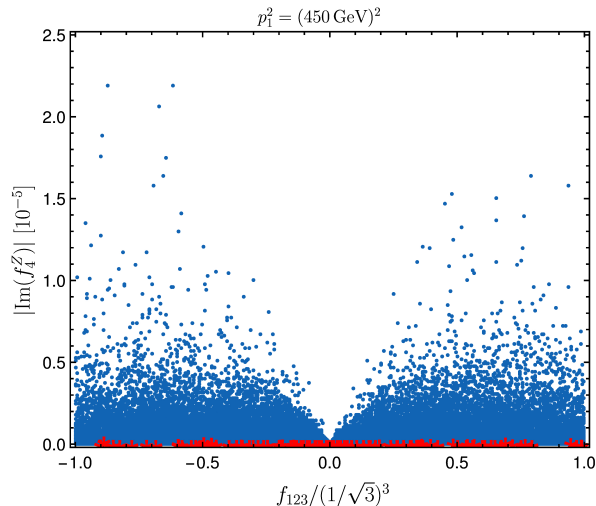


FIG. 6: Scatter plot for the imaginary part of f_4^Z for the ZW^+W^- vertex from Eq. (21), as a function of the combined Z -scalars coupling f_{123} , divided by its maximum possible value of $(1/\sqrt{3})^3$. The external Z boson 4-momentum is $p_1^2 = (450 \text{ GeV})^2$. In red, points for which the masses of all the dark neutral scalars are smaller than 200 GeV, $m_{h_i} < 200 \text{ GeV}$ ($i = 1, 2, 3$).

Interestingly, this form factor is larger, by roughly a factor of ten, than the corresponding quantity in the ZZZ vertex (though still smaller than the corresponding C2HDM typical values). This is illustrated in Fig. 6, where we plot the imaginary part of f_4^Z as given by Eq. (21) for $p_1^2 = (450 \text{ GeV})^2$, having obtained non-zero values. Therefore CPV also occurs in the ZW^+W^- interactions in this model, though presumably it would be no easier to experimentally establish than for the ZZZ vertex. The point we wished to make does not change, however – if even a single non-zero CPV quantity is found, then CP violation occurs in the model.

As an example of a possible experimental observable to which the form factors f_4^Z for the ZZZ interactions might contribute, let us take one of the asymmetries considered in Ref. [34], using the techniques of Ref. [71]. Considering a future linear collider and the process $e^+e^- \rightarrow ZZ$, taking cross sections for unpolarized beams $\sigma_{\lambda,\bar{\lambda}}$ for the production of two Z bosons of helicities λ and $\bar{\lambda}$ (assuming the helicity of the Z bosons can be determined), the asymmetry A_1^{ZZ} is defined as

$$A_1^{ZZ} = \frac{\sigma_{+,0} - \sigma_{0,-}}{\sigma_{+,0} + \sigma_{0,-}} = -4\beta\gamma^4 [(1 + \beta^2)^2 - 4\beta^2 \cos^2 \theta] \mathcal{F}_1(\beta, \theta) \text{Im}(f_4^Z(p_1^2)), \quad (22)$$

with θ the angle between the electron beam and the closest Z boson with positive helicity, $\beta = \sqrt{1 - 4m_Z^2/p_1^2}$ denoting the velocity of the produced Z bosons and the function $\mathcal{F}_1(\beta, \theta)$ is given in appendix D of Ref. [34]. Choosing the two points in our parameter scan with largest (positive) and smallest (negative) values of $\text{Im}(f_4^Z(p_1^2))$ for $p_1^2 = (450 \text{ GeV})^2$, we obtain the two curves shown in Fig. 7. Clearly, the smallness ($\sim 10^{-5}$) of the f_4^Z form factor renders the value of this asymmetry quite small, which makes its measurement challenging. This raises the possibility that asymmetries involving the ZW^+W^- vertex might be easier to measure than those pertaining to the ZZZ anomalous interactions, since we have shown that f_4^Z is typically larger by a factor of ten in the former vertex compared to the latter one. To investigate this possibility, we compared A_1^{ZZ} , considered above, with the A_1^{WW} asymmetry defined in Eq. (5.21) of Ref. [34]. A direct comparison of the maximum values of A_1^{WW} and A_1^{ZZ} shows that for some regions of parameter space the former quantity can indeed be one order of magnitude larger than the latter one; but that is by no means a generic feature, since for other choices of model parameters both asymmetries can also be of the same order. Notice that both asymmetries show a quite different \sqrt{s} dependence.

V. CONCLUSIONS

We presented a model whose scalar sector includes two Higgs doublets and a real singlet. A specific region of parameter space of the model yields a vacuum which preserves a discrete symmetry imposed on the model – thus a charged scalar and three neutral ones have a “dark” quantum number preserved in all interactions and have no interactions with fermions. The lightest of them, chosen to be a neutral particle, is therefore stable and a good dark

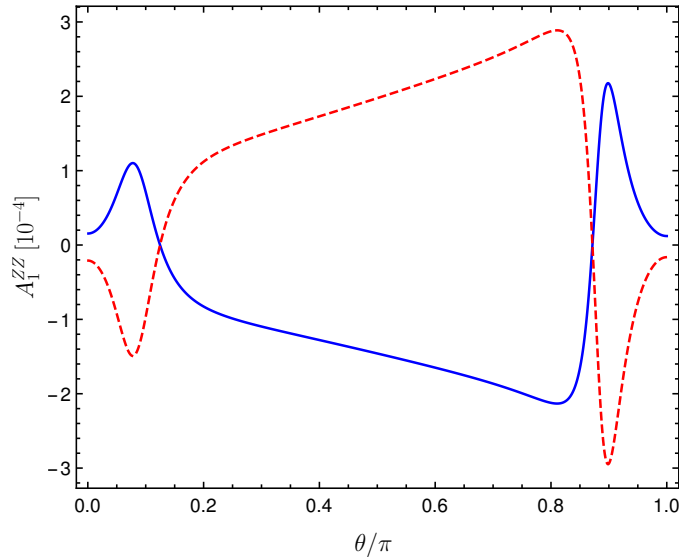


FIG. 7: The A_1^{ZZ} asymmetry of Eq. (22) as a function of the angle θ . The blue (full) curve corresponds to the largest positive value of $\text{Im}(f_4^Z(p_1^2))$ in our parameter scan, the red (dashed) one to the smallest negative value for the same quantity. In both cases, $p_1^2 = (450 \text{ GeV})^2$.

matter candidate. The first doublet yields the necessary Goldstone bosons and a neutral scalar which has automatically a behaviour almost indistinguishable from the SM Higgs boson. A parameter scan of the model, imposing all necessary theoretical and experimental constraints (including bounds due to relic density and dark matter searches, both direct and indirect) shows that the SM-like scalar state indeed complies with all known LHC data for the Higgs boson – some deviations may occur in the diphoton signal rate due to the extra contribution of a charged scalar to the involved decay width, but we have shown such deviations are at most roughly 20% of the expected SM result when all other constraints are satisfied, and this is still well within current experimental uncertainties.

The interesting thing about the model presented in this paper is the occurrence of explicit CP violation exclusively within the dark matter sector. A complex phase allowed in the potential forces the neutral components of the second (dark) doublet to mix with the real singlet to yield three neutral eigenstates, none of which possesses definite quantum numbers. Signals of this CP violation would not be observed in the fermion sector (which, by the way, we assume is identical to the one of the SM, and therefore has the usual CKM-type source of CP violation) nor in the interactions of the SM-like scalar – protected as it is by the unbroken Z_2 symmetry, and by the mass ranges chosen for the dark scalars, h will behave like a purely CP-even SM-like scalar, even though the CP symmetry of the model is explicitly broken in the scalar sector as well! Can the model then be said to be CP violating at all? The answer is yes, as an analysis of the contributions from the dark sector to the ZZZ vertex demonstrates. Even though the dark particles have no direct fermion interactions and could elude detection, their presence could be felt through the emergence of anomalous triple gauge boson vertices. Though we concentrated mainly on ZZZ vertices we also studied ZW^+W^- interactions, but our main purpose was to show CPV is indeed occurring. Direct measurements of experimental observables probing this CPV are challenging: we have considered a specific asymmetry, A_1^{ZZ} , built with ZZ production cross sections, but the magnitude of the CPV form factor f_4^Z yields extremely small values for that asymmetry, or indeed for other such variables we might construct. Direct measurements of ZZ production cross sections could in theory be used to constraint anomalous ZZZ vertex form factors – and indeed several experimental collaborations, from LEP, Tevatron and LHC, have tried that. But the experimentalists’ approach is based on constant and real form factors, whereas model-specific expressions for f_4^Z such as those considered in our work yield quantities highly dependent on external momenta, which boast sizeable imaginary parts as well. Thus a direct comparison with current experimental analyses is not conclusive.

The other remarkable fact is the amount of “damage” the mere inclusion of a real singlet can do to the model with two doublets. As repeatedly emphasised in the text, the model we considered is very similar to the Inert 2HDM – it is indeed simply the IDM with an added real singlet and a tweaked discrete symmetry, extended to the singlet having a “dark charge” as well. But whereas CP violation – explicit or spontaneous – is entirely impossible within the scalar sector of the IDM, the presence of the extra singlet produces a completely different situation. That one obtains a

model with explicit CPV is all the more remarkable when one considers that the field we are adding to the IDM is a *real* singlet, not even a complex one. Notice that within the IDM it is even impossible to tell which of the dark neutral scalars is CP-even and which is CP-odd – all that can be said is that those two eigenstates have opposite CP quantum numbers. The addition of a real singlet completely changes the CP picture.

The occurrence of CP violation in the dark matter sector can be simply a matter of curiosity, but one should not underestimate the possibility that something novel might arise from it. If the current picture of matter to dark matter abundance is indeed true and the observed matter is only 5% of the total content of the universe, then one can speculate how CP violation occurring in the interactions of the remainder matter might have affected the cosmological evolution of the universe. We reserve such studies for a follow-up work.

Acknowledgements

We acknowledge the contribution of the research training group GRK1694 ‘Elementary particle physics at highest energy and highest precision’. PF and RS are supported in part by the National Science Centre, Poland, the HARMONIA project under contract UMO-2015/18/M/ST2/00518. JW gratefully acknowledges funding from the PIER Helmholtz Graduate School.

-
- [1] G. Aad et al. (ATLAS), Phys. Lett. **B716**, 1 (2012), 1207.7214.
 - [2] S. Chatrchyan et al. (CMS), Phys. Lett. **B716**, 30 (2012), 1207.7235.
 - [3] G. Aad et al. (ATLAS, CMS), Phys. Rev. Lett. **114**, 191803 (2015), 1503.07589.
 - [4] G. Aad et al. (ATLAS, CMS), JHEP **08**, 045 (2016), 1606.02266.
 - [5] J. McDonald, Phys. Rev. **D50**, 3637 (1994), hep-ph/0702143.
 - [6] C. P. Burgess, M. Pospelov, and T. ter Veldhuis, Nucl. Phys. **B619**, 709 (2001), hep-ph/0011335.
 - [7] D. O’Connell, M. J. Ramsey-Musolf, and M. B. Wise, Phys. Rev. **D75**, 037701 (2007), hep-ph/0611014.
 - [8] O. Bahat-Treidel, Y. Grossman, and Y. Rozen, JHEP **05**, 022 (2007), hep-ph/0611162.
 - [9] V. Barger, P. Langacker, M. McCaskey, M. J. Ramsey-Musolf, and G. Shaughnessy, Phys. Rev. **D77**, 035005 (2008), 0706.4311.
 - [10] X.-G. He, T. Li, X.-Q. Li, and H.-C. Tsai, Mod. Phys. Lett. **A22**, 2121 (2007), hep-ph/0701156.
 - [11] H. Davoudiasl, R. Kitano, T. Li, and H. Murayama, Phys. Lett. **B609**, 117 (2005), hep-ph/0405097.
 - [12] L. Basso, O. Fischer, and J. J. van Der Bij, Phys. Lett. **B730**, 326 (2014), 1309.6086.
 - [13] O. Fischer (2016), 1607.00282.
 - [14] T. D. Lee, Phys. Rev. **D8**, 1226 (1973).
 - [15] G. C. Branco, P. M. Ferreira, L. Lavoura, M. N. Rebelo, M. Sher, and J. P. Silva, Phys. Rept. **516**, 1 (2012), 1106.0034.
 - [16] N. G. Deshpande and E. Ma, Phys. Rev. **D18**, 2574 (1978).
 - [17] R. Barbieri, L. J. Hall, and V. S. Rychkov, Phys. Rev. **D74**, 015007 (2006), hep-ph/0603188.
 - [18] L. Lopez Honorez, E. Nezri, J. F. Oliver, and M. H. G. Tytgat, JCAP **0702**, 028 (2007), hep-ph/0612275.
 - [19] E. M. Dolle and S. Su, Phys. Rev. **D80**, 055012 (2009), 0906.1609.
 - [20] L. Lopez Honorez and C. E. Yaguna, JHEP **09**, 046 (2010), 1003.3125.
 - [21] M. Gustafsson, S. Rydbeck, L. Lopez-Honorez, and E. Lundstrom, Phys. Rev. **D86**, 075019 (2012), 1206.6316.
 - [22] B. Swiezewska, Phys. Rev. **D88**, 055027 (2013), [Erratum: Phys. Rev.D88,no.11,119903(2013)], 1209.5725.
 - [23] B. Swiezewska and M. Krawczyk, Phys. Rev. **D88**, 035019 (2013), 1212.4100.
 - [24] A. Arhrib, Y.-L. S. Tsai, Q. Yuan, and T.-C. Yuan, JCAP **1406**, 030 (2014), 1310.0358.
 - [25] M. Klasen, C. E. Yaguna, and J. D. Ruiz-Alvarez, Phys. Rev. **D87**, 075025 (2013), 1302.1657.
 - [26] T. Abe, R. Kitano, and R. Sato, Phys. Rev. **D91**, 095004 (2015), [Erratum: Phys. Rev.D96,no.1,019902(2017)], 1411.1335.
 - [27] M. Krawczyk, D. Sokolowska, P. Swaczyna, and B. Swiezewska, JHEP **09**, 055 (2013), 1305.6266.
 - [28] A. Goudelis, B. Herrmann, and O. Stål, JHEP **09**, 106 (2013), 1303.3010.
 - [29] N. Chakrabarty, D. K. Ghosh, B. Mukhopadhyaya, and I. Saha, Phys. Rev. **D92**, 015002 (2015), 1501.03700.
 - [30] A. Ilnicka, M. Krawczyk, and T. Robens, Phys. Rev. **D93**, 055026 (2016), 1508.01671.
 - [31] A. Cordero-Cid, J. Hernández-Sánchez, V. Keus, S. F. King, S. Moretti, D. Rojas, and D. Sokolowska, JHEP **12**, 014 (2016), 1608.01673.
 - [32] D. Sokolowska, J. Phys. Conf. Ser. **873**, 012030 (2017).
 - [33] S. Moretti, Talk presented at Scalars 2017, Warsaw (2017).
 - [34] B. Grzadkowski, O. M. Ogreid, and P. Osland, JHEP **05**, 025 (2016), [Erratum: JHEP11,002(2017)], 1603.01388.
 - [35] H. Bélusca-Maïto, A. Falkowski, D. Fontes, J. C. Romão, and J. P. Silva, JHEP **04**, 002 (2018), 1710.05563.
 - [36] M. Mühlleitner, M. O. P. Sampaio, R. Santos, and J. Wittbrodt, JHEP **03**, 094 (2017), 1612.01309.
 - [37] S. L. Glashow and S. Weinberg, Phys. Rev. **D15**, 1958 (1977).
 - [38] E. A. Paschos, Phys. Rev. **D15**, 1966 (1977).
 - [39] G. C. Branco, L. Lavoura, and J. P. Silva, Int. Ser. Monogr. Phys. **103**, 1 (1999).

- [40] M. E. Peskin and T. Takeuchi, *Phys. Rev. Lett.* **65**, 964 (1990).
- [41] M. E. Peskin and T. Takeuchi, *Phys. Rev.* **D46**, 381 (1992).
- [42] I. Maksymyk, C. P. Burgess, and D. London, *Phys. Rev.* **D50**, 529 (1994), hep-ph/9306267.
- [43] G. Belanger, F. Boudjema, A. Pukhov, and A. Semenov, *Comput. Phys. Commun.* **176**, 367 (2007), hep-ph/0607059.
- [44] G. Belanger, F. Boudjema, A. Pukhov, and A. Semenov, *Comput. Phys. Commun.* **185**, 960 (2014), 1305.0237.
- [45] N. Aghanim et al. (Planck) (2018), 1807.06209.
- [46] E. Aprile et al. (XENON) (2018), 1805.12562.
- [47] R. Coimbra, M. O. P. Sampaio, and R. Santos, *Eur. Phys. J.* **C73**, 2428 (2013), 1301.2599.
- [48] I. Engeln, M. Mühlleitner, and J. Wittbrodt (2018), 1805.00966.
- [49] A. Djouadi, J. Kalinowski, and M. Spira, *Comput. Phys. Commun.* **108**, 56 (1998), hep-ph/9704448.
- [50] A. Djouadi, J. Kalinowski, M. Muehlleitner, and M. Spira (2018), 1801.09506.
- [51] M. Spira, *Fortsch. Phys.* **46**, 203 (1998), hep-ph/9705337.
- [52] M. Spira, *Prog. Part. Nucl. Phys.* **95**, 98 (2017), 1612.07651.
- [53] A. M. Sirunyan et al. (CMS) (2018), 1804.02716.
- [54] E. Aprile et al. (XENON), *Phys. Rev. Lett.* **119**, 181301 (2017), 1705.06655.
- [55] K. Hagiwara, R. D. Peccei, D. Zeppenfeld, and K. Hikasa, *Nucl. Phys.* **B282**, 253 (1987).
- [56] G. J. Gounaris, J. Layssac, and F. M. Renard, *Phys. Rev.* **D61**, 073013 (2000), hep-ph/9910395.
- [57] G. J. Gounaris, J. Layssac, and F. M. Renard, *Phys. Rev.* **D65**, 017302 (2002), [Phys. Rev.D62,073012(2000)], hep-ph/0005269.
- [58] U. Baur and D. L. Rainwater, *Phys. Rev.* **D62**, 113011 (2000), hep-ph/0008063.
- [59] T. Hahn and M. Perez-Victoria, *Comput. Phys. Commun.* **118**, 153 (1999), hep-ph/9807565.
- [60] L. Lavoura and J. P. Silva, *Phys. Rev.* **D50**, 4619 (1994), hep-ph/9404276.
- [61] F. J. Botella and J. P. Silva, *Phys. Rev.* **D51**, 3870 (1995), hep-ph/9411288.
- [62] T. Aaltonen et al. (CDF), *Phys. Rev. Lett.* **100**, 201801 (2008), 0801.4806.
- [63] T. Aaltonen et al. (CDF), *Phys. Rev. Lett.* **103**, 091803 (2009), 0905.4714.
- [64] V. M. Abazov et al. (D0), *Phys. Rev.* **D84**, 011103 (2011), 1104.3078.
- [65] V. M. Abazov et al. (D0), *Phys. Rev.* **D85**, 112005 (2012), 1201.5652.
- [66] G. Aad et al. (ATLAS), *Phys. Rev. Lett.* **108**, 041804 (2012), 1110.5016.
- [67] S. Chatrchyan et al. (CMS), *JHEP* **01**, 063 (2013), 1211.4890.
- [68] G. Aad et al. (ATLAS), *JHEP* **03**, 128 (2013), 1211.6096.
- [69] V. Khachatryan et al. (CMS), *Phys. Lett.* **B740**, 250 (2015), [erratum: Phys. Lett.B757,569(2016)], 1406.0113.
- [70] V. Khachatryan et al. (CMS), *Eur. Phys. J.* **C75**, 511 (2015), 1503.05467.
- [71] D. Chang, W.-Y. Keung, and P. B. Pal, *Phys. Rev.* **D51**, 1326 (1995), hep-ph/9407294.